

Exclusive heavy quark photoproduction in pp , pPb and $PbPb$ collisions at the LHC and FCC energies

V. P. Gonçalves, G. Sampaio dos Santos, C. R. Sena
*High and Medium Energy Group,
Instituto de Física e Matemática,
Universidade Federal de Pelotas
Caixa Postal 354, CEP 96010-900, Pelotas, RS, Brazil*
(Dated: November 12, 2019)

In this paper we present a comprehensive analysis of the exclusive heavy quark photoproduction in pp , pPb and $PbPb$ collisions at LHC and FCC energies using the Color Dipole formalism and taking into account of non-linear corrections to the QCD dynamics. We estimate the rapidity distributions and cross sections for the charm and bottom production considering the more recent phenomenological models for the dipole-proton scattering amplitude that are able to describe the ep HERA data. Our results indicate that a future experimental analysis of this process is feasible, which will allow us to improve our understanding of the QCD dynamics as well to perform the extraction of the elliptic component of the gluon Wigner distribution.

PACS numbers: 12.38.-t; 13.60.Le; 13.60.Hb

Keywords: Ultraperipheral Heavy Ion Collisions, Heavy Quark Production, QCD dynamics

I. INTRODUCTION

One of the main goals of Particle Physics is to achieve a deeper knowledge of the hadronic structure. A multidimensional partonic imaging of the hadron is provided by the 5-dimensional QCD Wigner distributions, which encode all quantum information about partons, including information on both generalized parton distributions (GPD) and transverse momentum dependent parton distributions (TMD) (See, e.g Refs. [1–4]). In the last years several authors proposed to constrain the gluon Wigner distribution in the nucleon by studying different final states that can be generated in photon-induced interactions present in electron-hadron and hadron-hadron collisions [5–13]. One of the more promising processes is the exclusive dijet photoproduction in ultraperipheral hadronic collisions [7], which are characterized by an impact parameter that is larger than the sum of the radius of the incident hadrons [14]. In such collisions the final state is very clean, being characterized by the dijet, two intact hadrons and two rapidity gaps associated to the photon and Pomeron exchanges. However, the measurement of the angular distribution of the Wigner distribution in this final state is challenging, since it requires reconstruction of full dijet kinematics. An alternative is to consider the exclusive heavy quark photoproduction in hadronic collisions [12]. As demonstrated for the first time in Ref. [15], such process probes the non-linear corrections to the QCD dynamics at high energies [16]. In order to reconstruct the isotropic and elliptic components of the gluon Wigner distribution, it is fundamental to access the dependence of the differential distribution in the relative quark-antiquark momentum for distinct values of the momentum transfer. Such analysis only will be feasible if the corresponding number of events generated in the current and/or future colliders is large. The main goal of this paper is to estimate the cross sections for the exclusive charm and bottom photoproduction in pp , pPb and $PbPb$ collisions considering the more recent phenomenological models for the dipole-proton scattering amplitude, which are based on the Color Glass Condensate formalism [17] and are able to describe the inclusive and exclusive ep HERA data. In our analysis we will present predictions for the rapidity distributions and cross sections for the LHC energies, which update the results presented in Ref. [15]. Moreover, predictions for the center-of-mass energies of the Future Circular Collider (FCC) [18] will be presented for the first time. Finally, a comparison between the predictions for the exclusive and inclusive heavy quark photoproduction also will be presented. As we will demonstrate below, our results indicate that a future experimental analysis of the exclusive heavy quark photoproduction is feasible and that this process can be used to improve our understanding of the QCD dynamics and constrain the elliptic component of the gluon Wigner function.

This paper is organized as follows. In the next Section we will present a brief review of the exclusive heavy quark photoproduction in hadronic collisions considering the Color Dipole formalism. In Section III we present our results for the rapidity distributions and cross sections in $pp/pPb/PbPb$ collisions at the LHC and FCC energies. Finally, in Section IV our main conclusions are summarized.

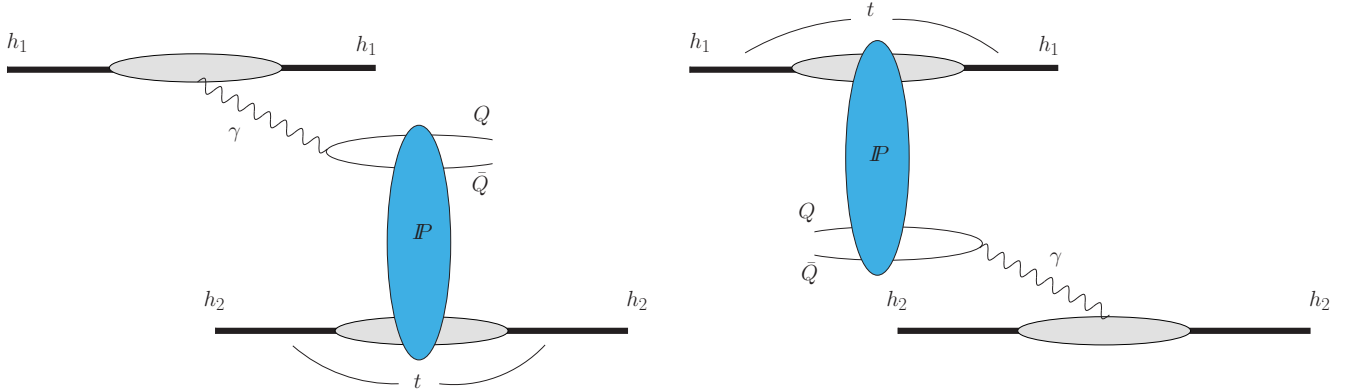


FIG. 1: Typical diagrams for the exclusive heavy quark photoproduction in a hadronic collision.

II. EXCLUSIVE HEAVY QUARK PHOTOPRODUCTION IN HADRONIC COLLISIONS

Let's initially present a brief review of the formalism (For more details see, e.g. Ref. [14]). In an ultraperipheral hadronic collision, in which the impact parameter is larger than the sum of the radius of the incident hadrons ($b > R_1 + R_2$), the photon-induced interactions become dominant. The typical diagrams for the heavy quark production in these reactions are presented in Fig. 1. The hadrons act as a source of almost real photons and the hadron-hadron cross section for the exclusive heavy quark photoproduction can be written in a factorized form, described using the equivalent photon approximation [14]. In particular, the differential cross section for the exclusive production of a heavy quark $Q\bar{Q}$ at rapidity Y will be given by

$$\frac{d\sigma [h_1 + h_2 \rightarrow h_1 + Q\bar{Q} + h_2]}{dY} = [n_{h_1}(\omega) \sigma_{\gamma h_2 \rightarrow Q\bar{Q} h_2} (W_{\gamma h_2}^2)]_{\omega_L} + [n_{h_2}(\omega) \sigma_{\gamma h_1 \rightarrow Q\bar{Q} h_1} (W_{\gamma h_1}^2)]_{\omega_R}, \quad (1)$$

where $\omega_L (\propto e^{+Y})$ and $\omega_R (\propto e^{-Y})$ denote photons from the h_1 and h_2 hadrons, respectively. The center-of-mass energy for the photon-hadron interactions is given by $W_{\gamma h} = \sqrt{4\omega E}$, where $E = \sqrt{s}/2$ and \sqrt{s} is the hadron-hadron c.m. energy. Moreover, $n(\omega)$ is the equivalent photon spectrum generated by the hadronic source, which we will assume to be described by the Drees-Zeppenfeld [19] and the relativistic point-like charge [14] models for the case of a proton and a nucleus, respectively. The exclusive heavy quark photoproduction cross section will be estimated using the Color Dipole formalism [20], which allows us to study the γh interaction in terms of a (color) dipole-hadron interaction and take into account of the non-linear effects in the QCD dynamics [16]. In this formalism, the photon-hadron cross section for the exclusive heavy quark production is given by

$$\sigma_{\gamma h \rightarrow Q\bar{Q} h} = \frac{1}{4} \int dz d^2\mathbf{r} |\Psi^T(z, \mathbf{r})|^2 \int d^2\mathbf{b}_h \left(\frac{d\sigma}{d^2\mathbf{b}_h} \right)^2, \quad (2)$$

where z is the photon momentum fraction carried by the quark, \mathbf{r} is the transverse dipole separation and \mathbf{b}_h is the impact parameter, given by the transverse distance between the centers of the dipole and the target. Moreover, for a transversely polarized photon with $Q^2 = 0$ one has that the squared wave function $|\Psi^T(z, \mathbf{r})|^2$ is given by [20]

$$|\Psi^T(z, \mathbf{r})|^2 = \frac{6 \alpha_{em} e_Q^2}{(2\pi)^2} \{m_Q^2 K_0^2(m_Q r) + m_Q^2 [z^2 + (1-z)^2] K_1^2(m_Q r)\}, \quad (3)$$

where e_Q is the fractional quark charge and m_Q the mass of the heavy quark. Furthermore, $x = 4m_Q^2/W_{\gamma h}^2$ and the differential dipole-hadron cross section can be expressed by

$$\frac{d\sigma}{d^2\mathbf{b}_h} = 2 \mathcal{N}_h(x, \mathbf{r}, \mathbf{b}_h), \quad (4)$$

where $\mathcal{N}_h(x, \mathbf{r}, \mathbf{b}_h)$ is the forward dipole-hadron scattering amplitude, which is dependent on the modelling of the QCD dynamics at high energies. As in our previous study [21], we will consider the bCGC [22] and IP-SAT [23] models for

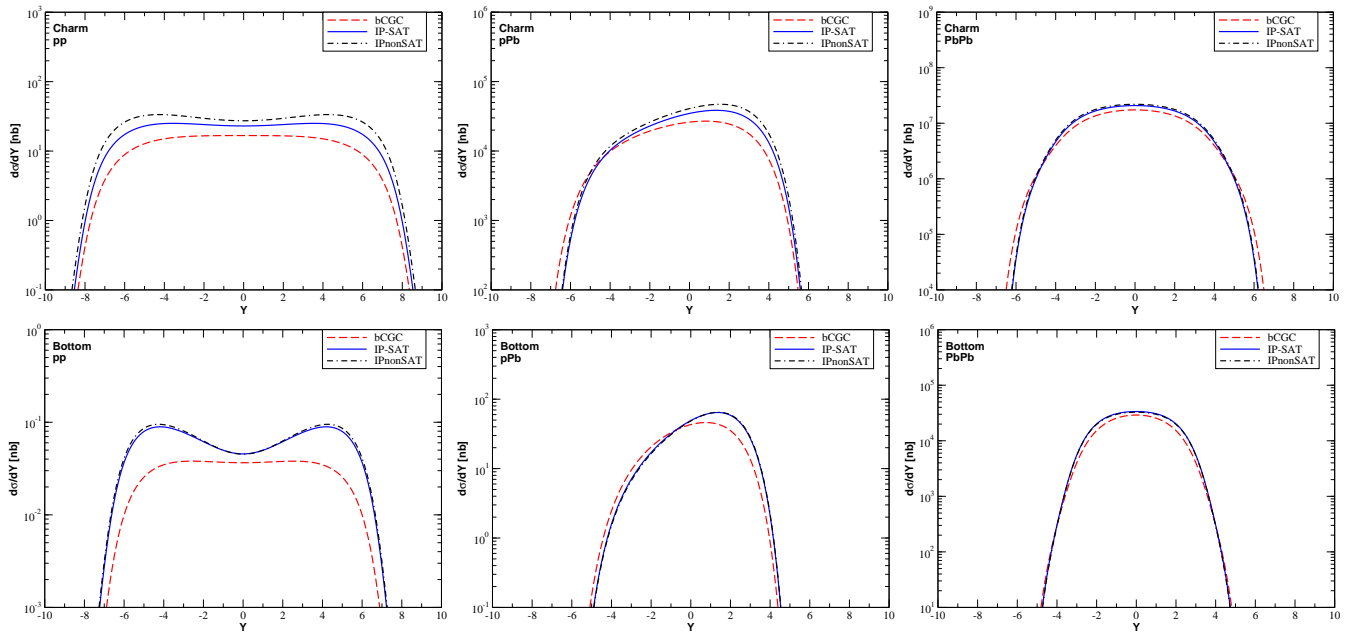


FIG. 2: Rapidity distributions for the exclusive charm (upper panels) and bottom (lower panels) photoproduction in pp ($\sqrt{s} = 13$ TeV), pPb ($\sqrt{s} = 8.1$ TeV) and $PbPb$ ($\sqrt{s} = 5.02$ TeV) collisions at the LHC.

the description of the dipole-proton scattering. Although these models differ in the treatment of the impact parameter dependence and/or of the linear and non-linear regimes, both describe quite well the high precision HERA data. One has that in the bCGC model, the linear regime of the dipole-proton scattering amplitude is described by the solution of the BFKL dynamics near of the saturation line, which implies that $\mathcal{N}_p \propto r^{2\gamma_{eff}}$ with $\gamma_{eff} \leq 1$. In contrast, the IP-SAT model predicts $\mathcal{N}_p \propto r^2 xg(x, 4/r^2)$ in the linear regime. On the other hand, the saturation regime is described in the bCGC model by the Levin-Tuchin law [24], while the IP-SAT predicts the saturation of \mathcal{N}_p at high energies and/or large dipoles, but the approach to this regime is not described by the Levin-Tuchin law. In our analysis we will assume for the bCGC model the set of parameters obtained in Ref. [25] by fitting the HERA data on the reduced ep cross sections. For the IP-SAT, we will assume the parameters obtained in Ref. [26]. In addition, we also will present the predictions derived using the IPnonSAT model proposed in Ref. [26], which is obtained disregarding the non-linear corrections in the IP-SAT model. The comparison between the IP-SAT and IPnonSAT predictions will allow us to estimate the impact of the non-linear corrections in the exclusive heavy quark photoproduction in hadronic colliders. For a nuclear target, we will assume that the dipole-nucleus scattering amplitude is given by

$$\mathcal{N}_A(x, \mathbf{r}, \mathbf{b}_A) = 1 - \exp \left[-\frac{1}{2} \sigma_{dp}(x, r^2) T_A(\mathbf{b}_A) \right], \quad (5)$$

where $T_A(\mathbf{b}_A)$ is the nuclear thickness, which is obtained from a 3-parameter Fermi distribution for the nuclear density normalized to A . Such model was proposed in Ref. [27] and is based on the Glauber-Mueller approach [28]. It is important to emphasize that such model describes the existing experimental data on the nuclear structure function [29]. We will compute \mathcal{N}_A considering the bCGC, IP-SAT and IPnonSAT models for the dipole-proton scattering amplitude discussed before.

III. RESULTS

In what follows we will present our predictions for the rapidity distribution and cross sections for the exclusive charm and bottom photoproduction in $pp/pPb/PbPb$ collisions at the LHC and FCC energies, obtained assuming $m_c = 1.27$ GeV and $m_b = 4.5$ GeV. We will consider the phenomenological dipole-proton models discussed above, which describe the ep HERA data. The comparison between the IP-SAT, IPnonSAT and bCGC predictions will allow us to estimate the impact of the non-linear effects, as well of the different descriptions of the transition between the linear and non-linear regimes. In Figs. 2 and 3 we present our results for the charm (upper panels) and bottom (lower panels) photoproduction in $pp/pPb/PbPb$ collisions at the LHC and FCC energies, respectively. Some comments are

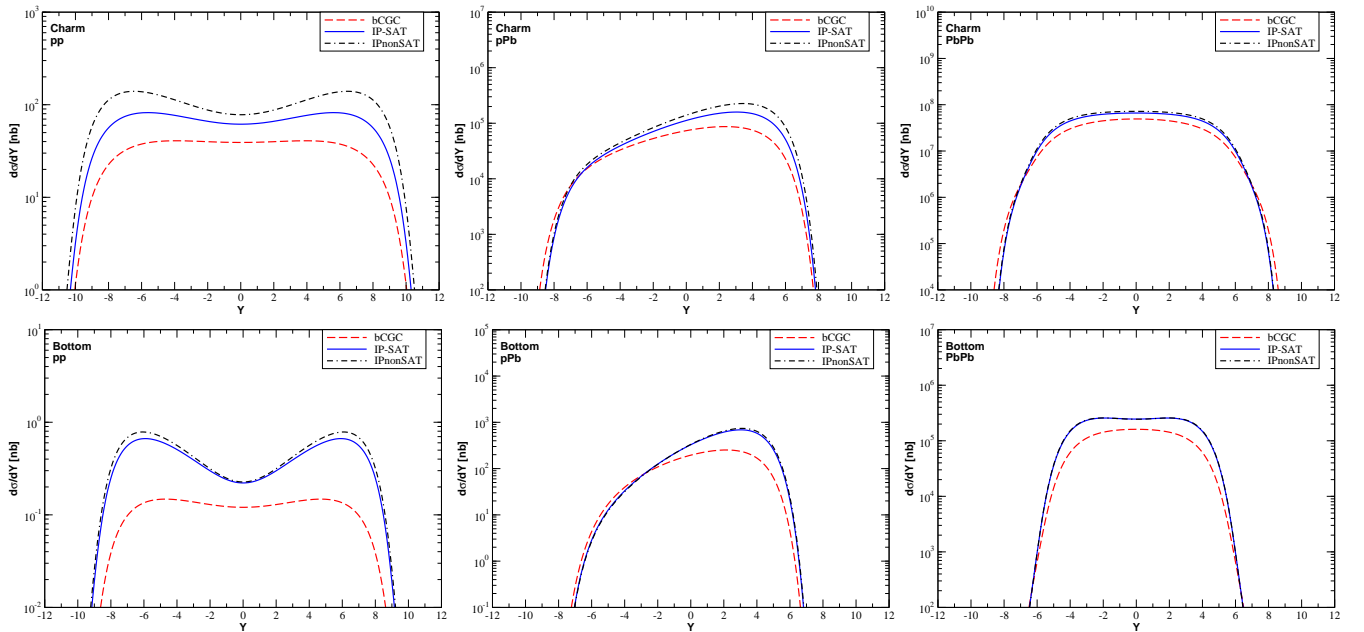


FIG. 3: Rapidity distributions for the exclusive charm (upper panels) and bottom (lower panels) photoproduction in pp ($\sqrt{s} = 100$ TeV), pPb ($\sqrt{s} = 63$ TeV) and $PbPb$ ($\sqrt{s} = 39$ TeV) collisions at the FCC.

in order. The distributions for pPb and $PbPb$ collisions are enhanced by a Z^2 factor, present in the nuclear photon flux. Moreover, the predictions for pPb collisions are asymmetric in rapidity due to the asymmetry on the initial photon fluxes associated to a proton and a nucleus, with the γh interactions being dominated by photons generated by the nucleus. Therefore, the behaviour of the distribution is determined by γp interactions with the photons emitted by the nucleus and the rapidity directly determines the value of x that is being probed: $x = 2m_Q e^{-Y}/\sqrt{s}$. For the heavy quark production, the cross sections are dominated by the interaction of dipoles of size $r \approx 1/m_Q$ (See e.g. Ref. [30]), i.e. the charm production is dominated by larger dipole sizes than for the bottom case. Consequently, the charm and bottom quark production probe \mathcal{N}_h at different values of r . In particular, the impact of the non-linear effects, which are important to large dipoles, is expected to decrease with the increasing of the heavy quark mass. Moreover, the contribution of the non-linear effects increases for the larger photon-hadron center-of-mass energies achieved at the FCC in comparison to the LHC. Such expectations are confirmed in the results presented in Figs. 2 and 3. We have that the difference between the IP-SAT and IPnonSAT predictions is negligible for bottom production, large for charm production and increases with the energy. One can also observe a large difference between the IP-SAT and bCGC predictions, which is directly related to distinct descriptions of the linear and non-linear regimes, as well as of the transition between these regimes discussed before. In particular, the large difference observed in the predictions for the bottom production in pp collisions is explained by the distinct treatments of the linear regime, which is dominated by the interaction of very small dipoles ($r \approx 1/m_b$) with the proton. Another way to observe these distinct treatments of the linear and non-linear regimes present in the phenomenological models is the analysis of the results for the charm production in pPb collisions. As pointed above, in this case the behaviour of the rapidity distribution is directly associated to the value that is being probed in the scattering amplitude. Therefore, for negative (positive) values of rapidity we are probing \mathcal{N}_p at large (small)- x . One have that bCGC prediction is larger than the IP-SAT one in the linear regime and smaller in the saturation regime. For $PbPb$ collisions, this difference is smaller, which is directly associated to the fact that we are using the Eq. (5) to describe the dipole-nucleus scattering, with the bCGC and IP-SAT only affecting the argument of the exponential.

In Tables I and II we present the corresponding predictions for the charm and bottom cross sections, respectively, considering the rapidity ranges probed by the CMS ($-2.5 \leq Y \leq +2.5$) and LHCb ($2.0 \leq Y \leq 4.5$) detectors. One have that the predictions for the LHCb range are approximately a factor ≥ 2 smaller than those for the CMS kinematical range. We predict large values for the event rates, in particular for the charm production in $PbPb$ collisions and FCC energies. The results indicate that a future measurement of the exclusive charm and bottom photoproduction in hadronic collisions is, in principle, feasible and that the analysis of this observable can be useful to constrain the description of the QCD dynamics at high energies. In addition, given the high values of the cross sections, we believe that the analysis of the differential distributions need to constrain the elliptic component of the gluon Wigner distribution could be performed in the forthcoming years.

	Rapidity range	bCGC	IP-SAT	IPnonSAT
pp ($\sqrt{s} = 13$ TeV)	$-2.5 < Y < 2.5$	83.24 nb	117.88 nb	142.70 nb
	$2 < Y < 4.5$	39.28 nb	61.85 nb	80.25 nb
pp ($\sqrt{s} = 100$ TeV)	$-2.5 < Y < 2.5$	197.64 nb	320.09 nb	415.05 nb
	$2 < Y < 4.5$	101.27 nb	181.68 nb	257.15 nb
pPb ($\sqrt{s} = 8.1$ TeV)	$-2.5 < Y < 2.5$	12.0×10^4 nb	16.2×10^4 nb	19.2×10^5 nb
	$2 < Y < 4.5$	3.69×10^4 nb	5.97×10^4 nb	7.70×10^4 nb
pPb ($\sqrt{s} = 63$ TeV)	$-2.5 < Y < 2.5$	3.58×10^5 nb	5.58×10^5 nb	7.08×10^5 nb
	$2 < Y < 4.5$	2.03×10^5 nb	3.83×10^5 nb	5.46×10^5 nb
PbPb ($\sqrt{s} = 5.02$ TeV)	$-2.5 < Y < 2.5$	7.70×10^7 nb	9.33×10^7 nb	9.87×10^7 nb
	$2 < Y < 4.5$	1.92×10^7 nb	2.35×10^7 nb	2.51×10^7 nb
PbPb ($\sqrt{s} = 39$ TeV)	$-2.5 < Y < 2.5$	2.35×10^8 nb	3.21×10^8 nb	3.50×10^8 nb
	$2 < Y < 4.5$	0.91×10^8 nb	1.30×10^8 nb	1.44×10^8 nb

TABLE I: Cross sections for the exclusive charm photoproduction in $pp/pPb/PbPb$ collisions at the LHC and FCC energies considering two rapidity ranges.

	Rapidity range	bCGC	IP-SAT	IPnonSAT
pp ($\sqrt{s} = 13$ TeV)	$-2.5 < Y < 2.5$	0.19 nb	0.27 nb	0.28 nb
	$2 < Y < 4.5$	0.09 nb	0.19 nb	0.21 nb
pp ($\sqrt{s} = 100$ TeV)	$-2.5 < Y < 2.5$	0.63 nb	1.31 nb	1.36 nb
	$2 < Y < 4.5$	0.35 nb	1.06 nb	1.16 nb
pPb ($\sqrt{s} = 8.1$ TeV)	$-2.5 < Y < 2.5$	176.06 nb	217.53 nb	216.50 nb
	$2 < Y < 4.5$	30.59 nb	57.16 nb	58.73 nb
pPb ($\sqrt{s} = 63$ TeV)	$-2.5 < Y < 2.5$	937.47 nb	1750.20 nb	1804.24 nb
	$2 < Y < 4.5$	527.13 nb	1572.13 nb	1696.10 nb
PbPb ($\sqrt{s} = 5.02$ TeV)	$-2.5 < Y < 2.5$	10.1×10^4 nb	13.4×10^4 nb	13.3×10^4 nb
	$2 < Y < 4.5$	1.09×10^4 nb	1.47×10^4 nb	1.44×10^4 nb
PbPb ($\sqrt{s} = 39$ TeV)	$-2.5 < Y < 2.5$	7.6×10^5 nb	12.6×10^5 nb	12.7×10^5 nb
	$2 < Y < 4.5$	2.41×10^5 nb	5.04×10^5 nb	5.12×10^5 nb

TABLE II: Cross sections for the exclusive bottom photoproduction in $pp/pPb/PbPb$ collisions at the LHC and FCC energies considering two rapidity ranges.

Finally, let's compare the predictions for the charm and bottom photoproduction in inclusive and exclusive processes, derived using the IP-SAT model. In contrast to the exclusive case, in inclusive interactions one of the incident hadrons fragments and the photon-hadron cross section is linearly proportional to $d\sigma/d^2\mathbf{b}_h$ (For details see, e.g. [21]). In Figs. 4 and 5 we present our results for $pp/pPb/PbPb$ collisions at the LHC and FCC energies, respectively. The results for charm (bottom) production are presented in the upper (lower) panels. In the case of charm production in pp and pPb collisions at the LHC, we have that the exclusive prediction is a factor $\mathcal{O}(20)$ smaller than the inclusive one for midrapidities. On the other hand, for $PbPb$ collisions, this factor is $\mathcal{O}(10)$. For the FCC we have that the corresponding factors are of order of 15/18/8 for $pp/pPb/PbPb$ collisions, respectively. In contrast, we have that exclusive bottom photoproduction is a factor $\mathcal{O}(100)$ [$\mathcal{O}(80)$] smaller than the inclusive one for the LHC [FCC] energies. It is important to emphasize that the free parameters present in the Color Dipole formalism have been constrained by the HERA data, which implies that our predictions are parameter free. Moreover, as the inclusive and exclusive photoproduction in hadronic collisions are determined by the same quantities, i.e. the photon wave function and the color-dipole amplitude, a future measurement of both processes will be an important test of the universality of the Color Dipole formalism as well of the treatment of the non-linear corrections to the QCD dynamics.

IV. SUMMARY

In summary, we have computed the rapidity distributions and cross sections for the exclusive charm and bottom photoproduction in $pp/pPb/PbPb$ collisions at the LHC and FCC energies. Our study was motivated by the possibility of use this process to constrain the elliptic component of the gluon Wigner distribution by the analysis of the differential distribution in the relative quark-antiquark momentum for distinct values of the momentum transfer. Our predictions indicate that the expected number of events is very large, in particular for charm production in $PbPb$ collisions at

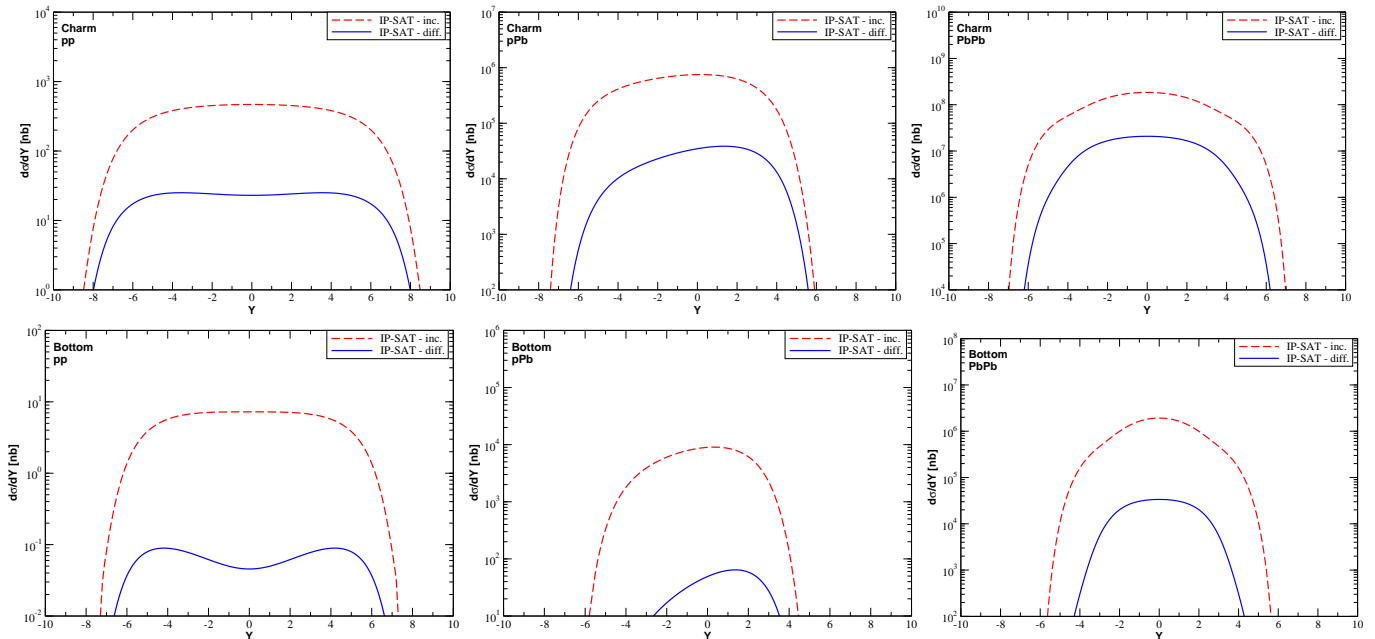


FIG. 4: Comparison between the rapidity distributions for the inclusive and exclusive charm (upper panels) and bottom (lower panels) photoproduction in pp ($\sqrt{s} = 13$ TeV), pPb ($\sqrt{s} = 8.1$ TeV) and $PbPb$ ($\sqrt{s} = 5.02$ TeV) collisions at the LHC.

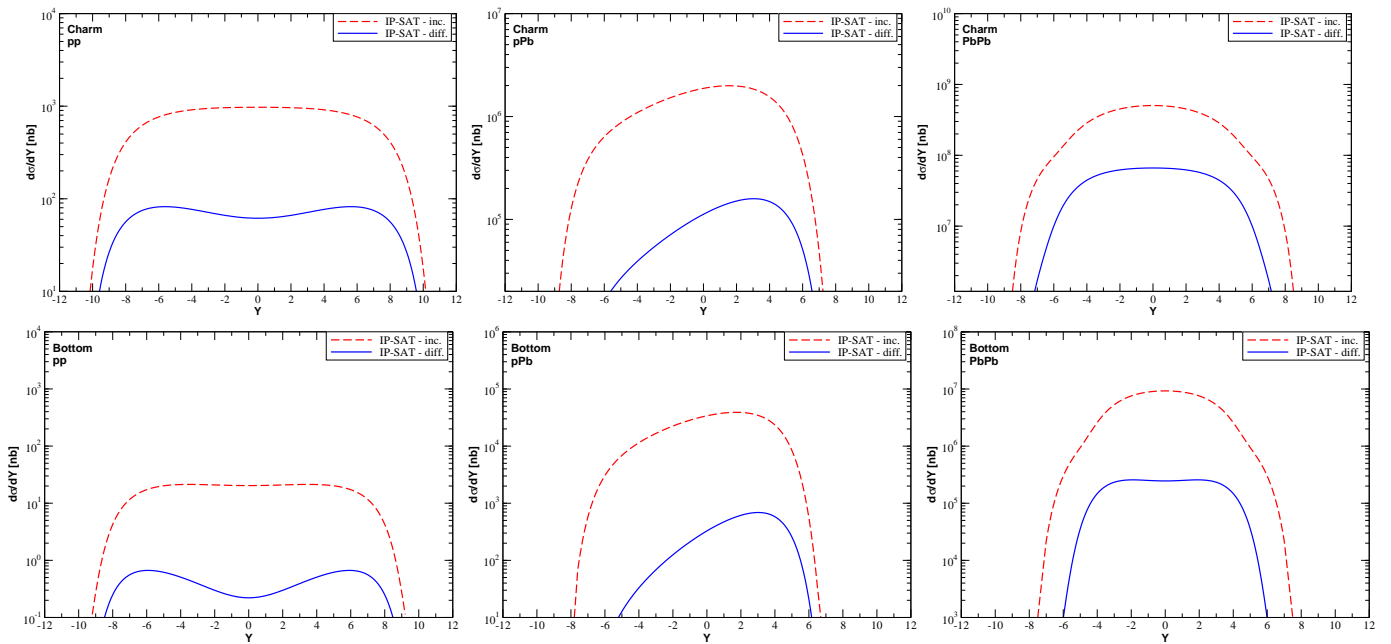


FIG. 5: Comparison between the rapidity distributions for the inclusive and exclusive charm (upper panels) and bottom (lower panels) photoproduction in pp ($\sqrt{s} = 100$ TeV), pPb ($\sqrt{s} = 63$ TeV) and $PbPb$ ($\sqrt{s} = 39$ TeV) collisions at the FCC.

the FCC. Therefore, we strongly recommend a future experimental analysis of this process in order to improve our understanding of the QCD dynamics and to access the gluon Wigner distribution.

Acknowledgements

VPG would like to express a special thanks to the Mainz Institute for Theoretical Physics (MITP) of the Cluster of Excellence PRISMA+ (Project ID 39083149) for its hospitality and support. This work was partially financed by the Brazilian funding agencies CAPES, CNPq, FAPERGS and INCT-FNA (process number 464898/2014-5).

-
- [1] X. d. Ji, Phys. Rev. Lett. **91**, 062001 (2003)
 - [2] M. Diehl, Phys. Rept. **388**, 41 (2003)
 - [3] D. Boer *et al.*, arXiv:1108.1713 [nucl-th].
 - [4] Y. Hagiwara, Y. Hatta and T. Ueda, Phys. Rev. D **94**, no. 9, 094036 (2016)
 - [5] Y. Hatta, B. W. Xiao and F. Yuan, Phys. Rev. Lett. **116**, no. 20, 202301 (2016)
 - [6] T. Altinoluk, N. Armesto, G. Beuf and A. H. Rezaeian, Phys. Lett. B **758**, 373 (2016)
 - [7] Y. Hagiwara, Y. Hatta, R. Pasechnik, M. Tasevsky and O. Teryaev, Phys. Rev. D **96**, no. 3, 034009 (2017)
 - [8] R. Boussarie, Y. Hatta, B. W. Xiao and F. Yuan, Phys. Rev. D **98**, no. 7, 074015 (2018)
 - [9] H. Mantysaari, N. Mueller and B. Schenke, Phys. Rev. D **99**, no. 7, 074004 (2019)
 - [10] F. Salazar and B. Schenke, Phys. Rev. D **100**, no. 3, 034007 (2019)
 - [11] R. Boussarie, A. V. Grabovsky, L. Szymanowski and S. Wallon, Phys. Rev. D **100**, no. 7, 074020 (2019)
 - [12] M. Reinke Pelicer, E. Grave De Oliveira and R. Pasechnik, Phys. Rev. D **99**, no. 3, 034016 (2019)
 - [13] Y. Hatta, N. Mueller, T. Ueda and F. Yuan, arXiv:1907.09491 [hep-ph].
 - [14] C. A. Bertulani and G. Baur, Phys. Rep. **163**, 299 (1988); F. Krauss, M. Greiner and G. Soff, Prog. Part. Nucl. Phys. **39**, 503 (1997).; G. Baur, K. Hencken and D. Trautmann, J. Phys. G **24**, 1657 (1998); G. Baur, K. Hencken, D. Trautmann, S. Sadovsky, Y. Kharlov, Phys. Rep. **364**, 359 (2002); C. A. Bertulani, S. R. Klein and J. Nystrand, Ann. Rev. Nucl. Part. Sci. **55**, 271 (2005); V. P. Goncalves and M. V. T. Machado, J. Phys. G **32**, 295 (2006); A. J. Baltz *et al.*, Phys. Rept. **458**, 1 (2008); J. G. Contreras and J. D. Tapia Takaki, Int. J. Mod. Phys. A **30**, 1542012 (2015).
 - [15] V. P. Goncalves and M. V. T. Machado, Phys. Rev. D **75**, 031502 (2007)
 - [16] F. Gelis, E. Iancu, J. Jalilian-Marian and R. Venugopalan, Ann. Rev. Nucl. Part. Sci. **60**, 463 (2010); H. Weigert, Prog. Part. Nucl. Phys. **55**, 461 (2005); J. Jalilian-Marian and Y. V. Kovchegov, Prog. Part. Nucl. Phys. **56**, 104 (2006).
 - [17] J. Jalilian-Marian, A. Kovner, L. McLerran and H. Weigert, Phys. Rev. D **55**, 5414 (1997); J. Jalilian-Marian, A. Kovner and H. Weigert, Phys. Rev. D **59**, 014014 (1999); Phys. Rev. D **59**, 014015 (1999); Phys. Rev. D **59**, 034007 (1999); E. Iancu, A. Leonidov and L. McLerran, Nucl. Phys. **A692**, 583 (2001); E. Ferreira, E. Iancu, A. Leonidov and L. McLerran, Nucl. Phys. **A701**, 489 (2002); H. Weigert, Nucl. Phys. **A703**, 823 (2002).
 - [18] A. Abada *et al.* [FCC Collaboration], Eur. Phys. J. C **79**, no. 6, 474 (2019); Eur. Phys. J. ST **228**, no. 4, 755 (2019); Eur. Phys. J. ST **228**, no. 5, 1109 (2019).
 - [19] M. Drees and D. Zeppenfeld, Phys. Rev. D **39**, 2536 (1989).
 - [20] N. N. Nikolaev, B. G. Zakharov, Phys. Lett. B **332**, 184 (1994); Z. Phys. C **64**, 631 (1994).
 - [21] V. P. Goncalves, G. Sampaio dos Santos and C. R. Sena, Nucl. Phys. A **976**, 33 (2018)
 - [22] H. Kowalski, L. Motyka and G. Watt, Phys. Rev. D **74**, 074016 (2006).
 - [23] H. Kowalski and D. Teaney, Phys. Rev. D **68**, 114005 (2003).
 - [24] E. Levin and K. Tuchin, Nucl. Phys. A **691**, 779 (2001)
 - [25] A. H. Rezaeian and I. Schmidt, Phys. Rev. D **88**, 074016 (2013)
 - [26] H. Mantysaari and P. Zurita, Phys. Rev. D **98**, 036002 (2018)
 - [27] N. Armesto, Eur. Phys. J. C **26**, 35 (2002).
 - [28] A. H. Mueller, Nucl. Phys. B **335**, 115 (1990).
 - [29] E. R. Cazaroto, F. Carvalho, V. P. Goncalves and F. S. Navarra, Phys. Lett. B **671**, 233 (2009)
 - [30] M. S. Kugeratski, V. P. Goncalves and F. S. Navarra, Eur. Phys. J. C **46**, 465 (2006); Eur. Phys. J. C **46**, 413 (2006)